Supplemental Information:

Non-coding transcription is a driving force of nucleosome instability in *spt16* mutant cells

Jianxun Feng[#1,4], Haiyun Gan[#2], Matthew L. Eaton[3], Hui Zhou[2], Shuqi Li[4], David M. MacAlpine[3], and Zhiguo Zhang[*2] and Qing Li[*1,4]

[1]State Key Laboratory of Protein and Plant Gene Research, School of Life Sciences and Peking-Tsinghua Center for Life Sciences

Peking University

Beijing, China 100871

[2]Department of Biochemistry and Molecular Biology

Mayo Clinic College of Medicine

200 First Street SW

Rochester, MN 55905

[3]Department of Pharmacology and Cancer Biology

Duke University Medical Center,

Durham, North Carolina 27710

[4]Academy for Advanced Interdisciplinary Studies, Peking University

[#]These authors contributed equally to this work

*Corresponding author: Zhiguo Zhang (Zhang.Zhiguo@mayo.edu) and Qing Li (li.qing@pku.edu.cn)

Phone: 507-538-6074, 86-10-62752516 Fax: 507-284-9759

Running title: A vicious cycle of cryptic transcription and nucleosome instability

Supplemental Figures

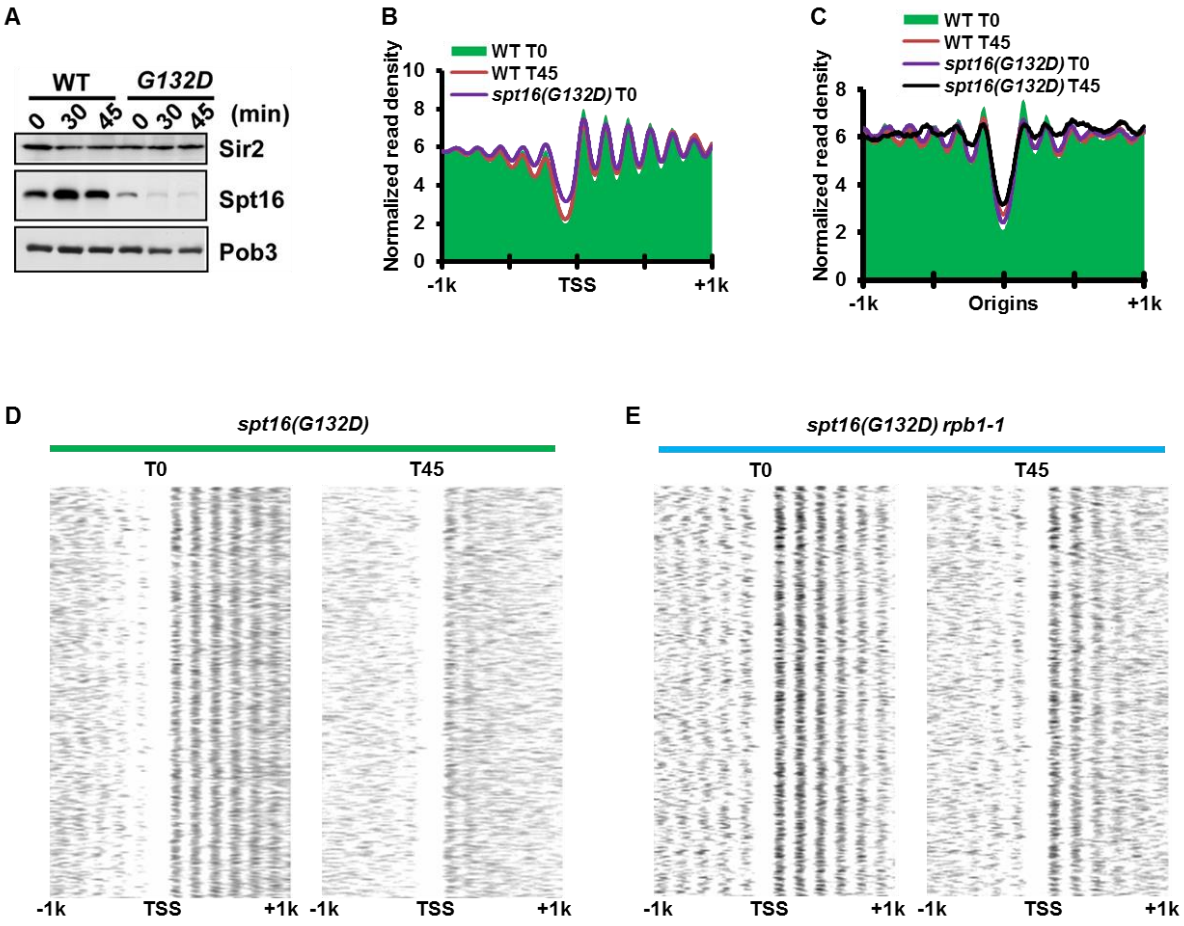

FIG S1. Inactivation of Spt16 results in global nucleosome changes. (A) Spt16 is depleted in *spt16 (G132D)*, but not in wild type cells at 37ºC. WT and *spt16 (G132D)* cells were arrested at 25ºC (0) and shifted to 37 ºC for 30 min or 45 min. Whole cell extracts were prepared for Western blot analysis of Spt16, Pob3 and Sir2 (loading control). (B) The average nucleosome organization around the transcription start sites (TSS) in wild type (WT) cells at 25ºC (T0) and at 37ºC for 45 min (T45) and *spt16 (G132D)* at 37ºC for 0 min (T0) were shown. Cells were arrested to G1 phase (T0) and then shift to 37ºC for 45 min for nucleosome mapping using MNase-seq. We performed nucleosome mapping at G1 to avoid complication of cell cycle on nucleosomal changes.

(C) Inactivation of *spt16* results in global loss of nucleosomes at DNA replication origins. The nucleosome mapping was performed as (B) and DNA replication origins dataset was from (1). (D-E) Heat map of nucleosome occupancy at TSS sites in *spt16 (G132D)* mutant cells (D) and *spt16 (G132D) rpb1-1* mutant cells (E) at 25^{o}C (T0) and at 37^{o}C for 45 min (T45) were shown. Each row represents one ORF. A 4bp window was used to scan the reads density of MNase-seq from 1Kb downstream to 1Kb upstream of TSS. Dark color represents regions with organized nucleosomes.

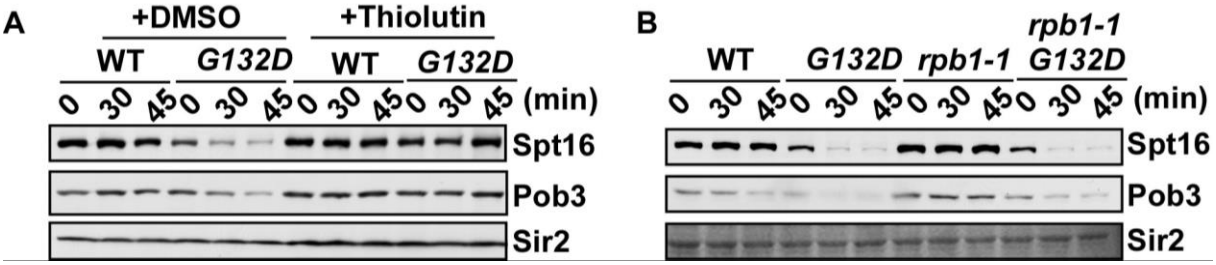

FIG S2. The drug thiolutin and the *rbp1-1* mutant have different effect on Spt16 depletion. (A) Thiolutin inhibits the depletion of Spt16 (G132D) proteins at non-permissive temperature compared to mock treated cells. Wild type (WT) and *spt16 (G132D)* mutant cells were synchronized at G1 using α–factor and then treated with thiolutin or DMSO (mock) for 15 min before shifting to the non-permissive temperature (37^{o}C). At the indicated time points after temperature shift (37^{o}C), cells were collected for analysis of protein levels by Western blot. (B) Inhibition of *rbp1-1* at non-permissive temperature does not affect *spt16 (G132D)* depletion. The experiments were performed as described above except that different mutants were used with DMSO treatment.

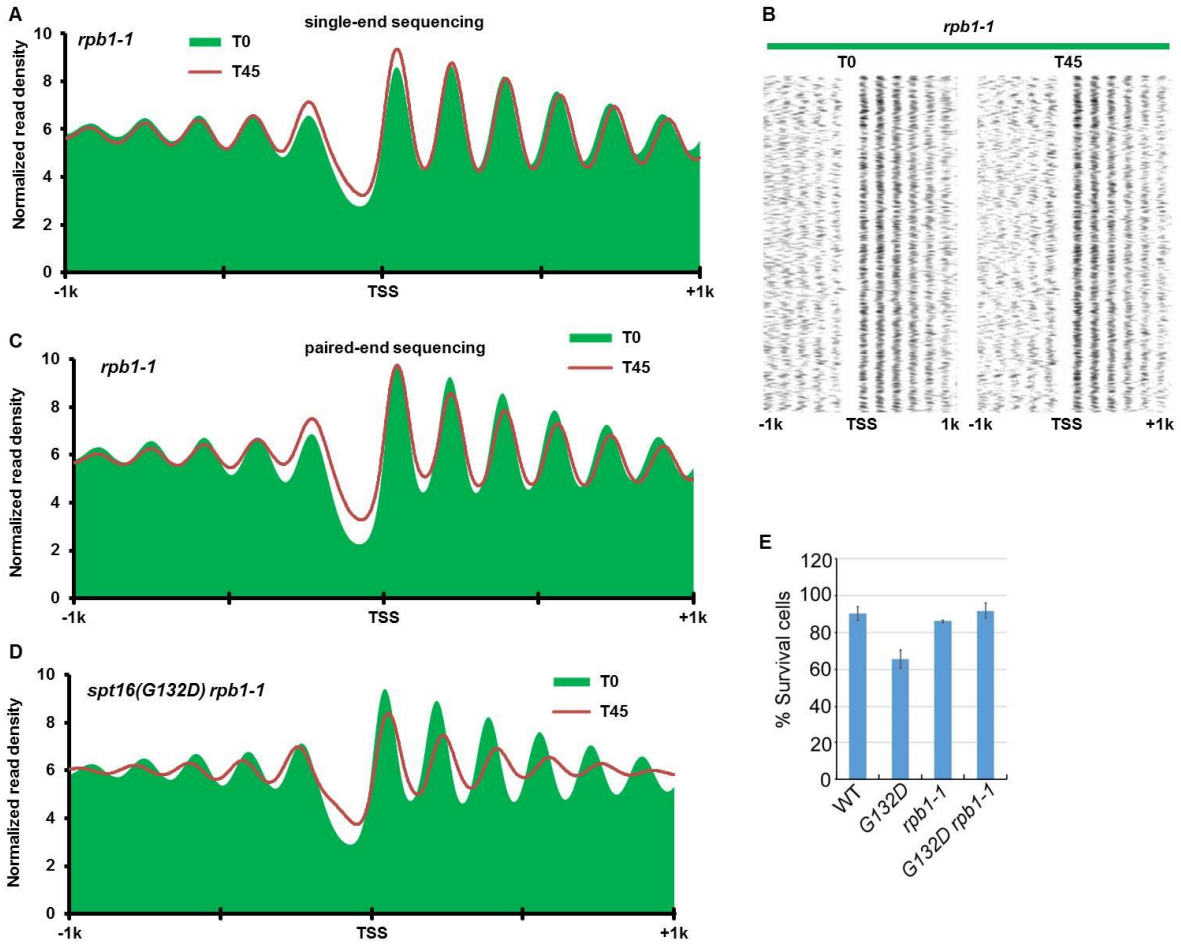

FIG S3. Nucleosomes in *rbp1-1* cells shifted slightly towards TES at non-permissive temperature. (A) The average nucleosome occupancy surrounding TSS in *rpb1-1* mutant cells at 37ºC for 0 min (T0, green) and for 45 min (T45, red line) was calculated. (B) Heat map of nucleosome occupancy at TSS sites in *rpb1-1* mutant cells. *rpb1-1* mutant cells at permissive temperature 37ºC (T0) and 37ºC treatment for 45 minutes (red line, T45) were shown. Nucleosome heat map was generated using method described in Fig. S1D-E. (C-D) The average nucleosome organization around the transcription start sites (TSS) in *rpb1-1* (C) and *spt16 (G132D) rpb1-1* (D) mutant

cells based on analysis of Mnase-seq datasets using paired-end sequencing. (E) Inhibition of *rbp1-1* restores the reduced cell viability of *spt16(G132D)* cells at non-permissive temperature. Cells arrested at G1 phase using α factor 25^{o}C were either treated at 37^{o}C for 45 min or left at 25^{o}C for 45 min. These cells were then diluted and plated onto YPD plates. These plates were incubated at 25^{o}C for 2-3 days. Colonies were counted, and relative viability was calculated by the number of colonies formed from cells treated with 37^{o}C divided by that formed at 25^{o}C . Three plates were used for each sample at each time point for technical repeats. In addition, two biological repeats were performed. The results were from the average and SD from 6 repeats.

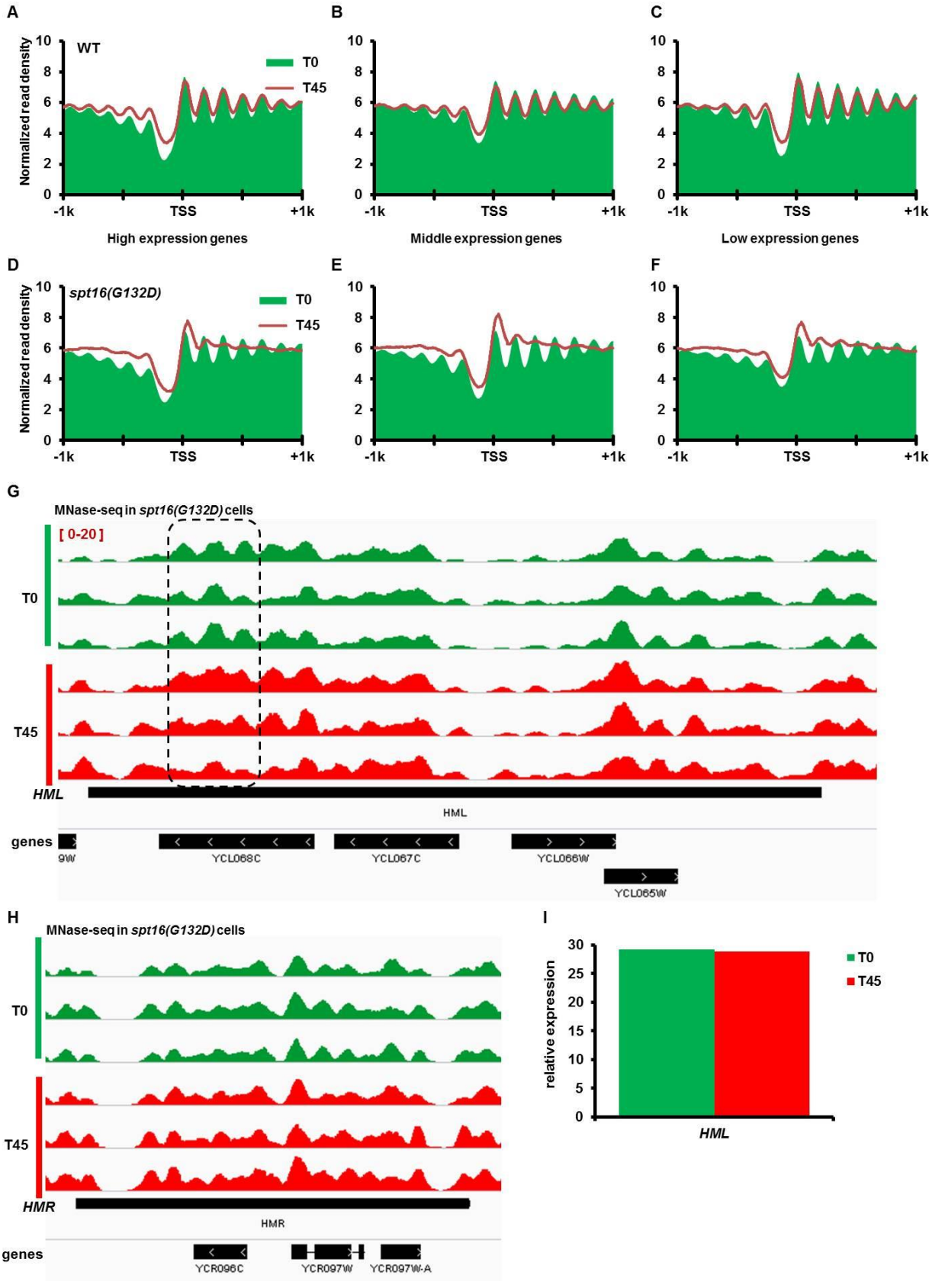
A
B
C
WT
T0
T45
Normalized read density
-1k
TSS
+1k
High expression genes
Middle expression genes
Low expression genes
D
E
F
spt16(G132D)
G
MNase-seq in spt16(G132D) cells
[0-20]
T0
T45
HML
genes
9W
YCL068C
YCL067C
YCL066W
YCL065W
H
MNase-seq in spt16(G132D) cells
HMR
YCR096C
YCR097W
YCR097W-A
I
relative expression
HML

FIG S4. Nucleosome loss at gene body in *spt16 (G132D)* cells is independent of expression levels of coding genes. (A-F) The average nucleosome positioning surrounding transcription start site (TSS) of genes with high, middle and low expression for WT cells (A-C) and *spt16 (G132D)* cells (D-F) were calculated using similar procedures described in Fig. 1. The entire yeast genes were divided into three groups based on the reported transcript abundance (2). (G) Nucleosomes at the silent *HML* locus were altered in *spt16 (G132D)* cells at 37ºC for 45 min. MNase-seq sequence reads at the *HML* locus from three independent experiments at permissive temperature (T0) and 37°C for 45 min (T45) were shown. The grey box highlights a region with altered nucleosome positions. (H) Nucleosomes at the *HMR* locus were not altered in *spt16 (G132D)* cells at 37ºC for 45 min. (I) The expression of the two genes at silent *HML* locus were not altered in *spt16 (G132D)* cells at 37ºC for 45 min. RNA-seq reads were used to calculated the relative gene expression of $\alpha 1$ and $\alpha 2$ genes at the *HML* locus at two different temperature. Since RNA-seq results were obtained using *MATa* strain and we did not calculate the expression of *HMR* locus.

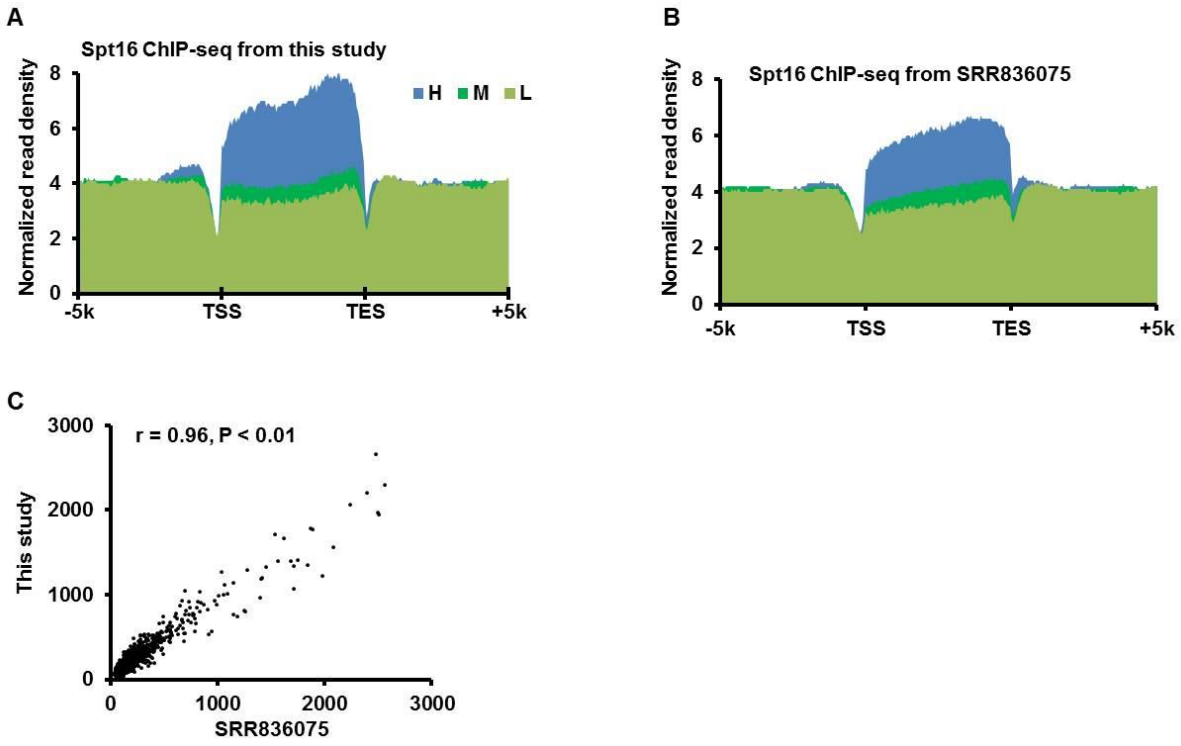

FIG S5. Spt16 is enriched at highly expressed genes. The average read density of Spt16 ChIP-seq from this study (A) or public work (3) (B) from 5Kb upstream TSS to 5Kb downstream of TES was calculated. The entire yeast genes were split into three groups according to their expression status described in Fig. 2 and Fig. S1A. H: high, M: middle, and L: low expression. (C) Correlation of Spt16 ChIP-seq result between this study and the public work. The Spt16 peaks were identified by MACS2 and used to perform dot plot, and correlation analysis (Pearson's correlation coefficient) was calculated.

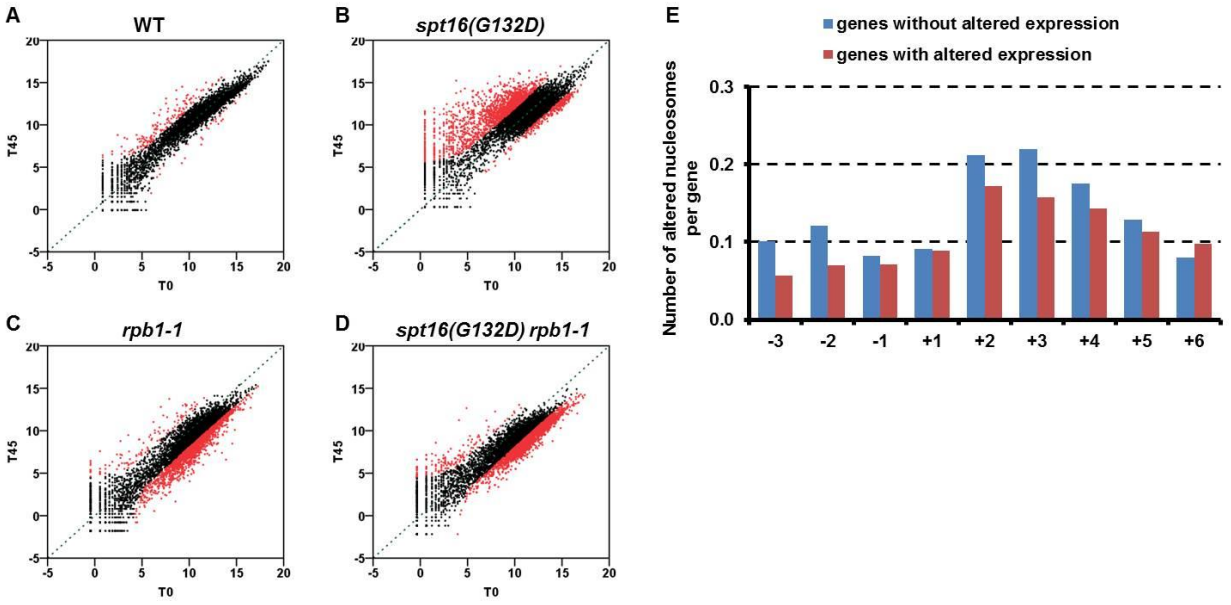

FIG S6. The transcription of some coding gene is changed upon depletion of Spt16. (A-D) Effect of inactivation of *spt16 (G132D)* (B), *rpb1-1* (C) alone or in combination (D) on transcription of coding genes. The dot plot shows the variation of the $\log_2$ ratio of RPKM at 45min (T45) over 0min (T0) of individual ORFs in WT (A), *spt16 (G132D)* (B), *rpb1-1* (C), and *spt16 (G132D) rpb1-1* (D) mutation cells. Each dot represents one ORF, and the red dots represent ORFs that exhibit a significant change (calculated by DE seq (4)) in gene expression. (E) The nucleosomal changes at genes with changed expression upon Spt16 depletion are similar to those without changed expression. Genes were separated into two groups based on whether their expression was altered in *spt16 (G132D)* cells shown in (B). The number of altered nucleosomes per gene from -3 to +6 nucleosome positions of each ORF after TSS (X-axis) was calculated (Y-axis).

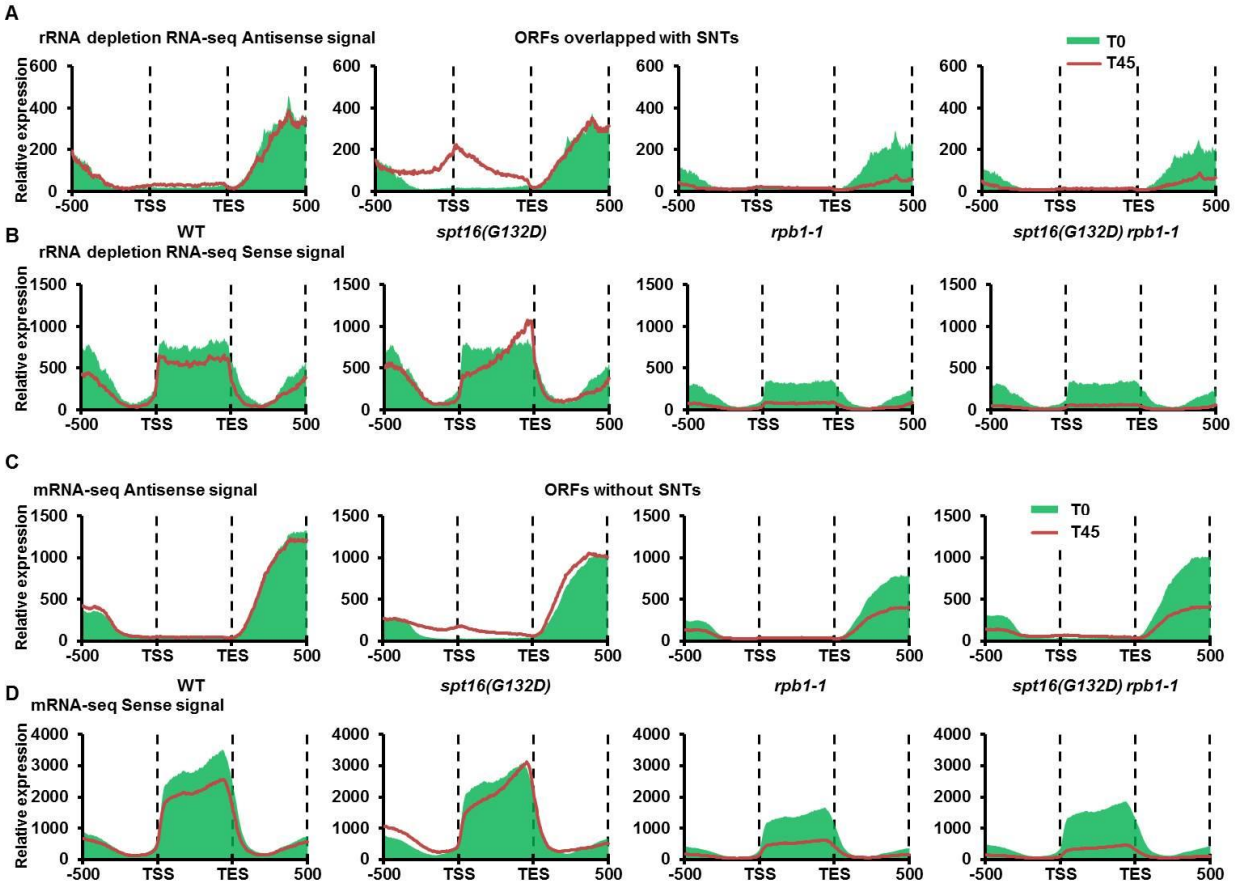

FIG S7. The transcription status of ORFs overlapped with or without SNTs. (A-B) Both antisense (A) and sense (B) non-coding transcripts increase at ORFs overlapped with SNTs in the *spt16 (G132D)* mutant cells detected RNA-seq using rRNA depletion RNA. (C-D) Neither the antisense nor sense transcripts are altered to a significant degree at ORFs without SNTs upon depletion of Spt16. The antisense (C) and sense (D) RNA-seq reads of ORFs without SNTs calculated using similar procedures described in Fig. 4E-F and were plotted from 500 bp upstream of TSS to 500 bp downstream of TES. WT, *spt16 (G132D)*, *rpb1-1*, and *spt16 (G132D) rpb1-1* mutation cells before and after restrictive temperature treatments were plotted as green areas (T0) and red lines (T45), respectively.

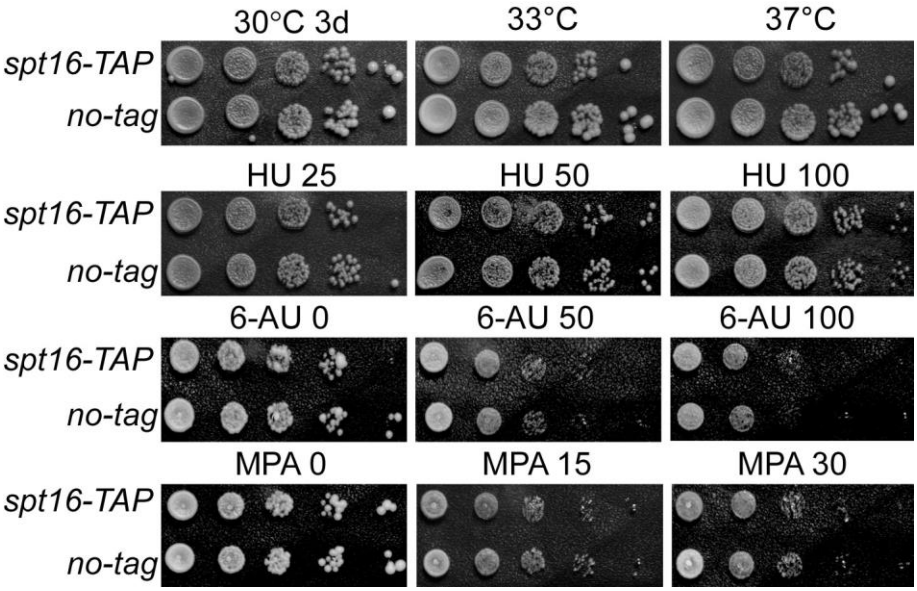

FIG S8. Spt16-TAP is functional. Ten-fold serial dilution of WT (no-tag) strain and the strain expressing Spt16-TAP were spotted YPD plates (different temperatures) or with plates containing different concentrations hydroxyurea (HU), 6-Azauracil (6-AU) and mycophenolic acid (MPA). These plates were then incubated at 30^{o}C for 2-3 days before photography. Number indicates the concentration used for the study: HU (mM); 6-AU and MPA (μg/ml).

Table S1: Correlation of Mnase-seq repeats and RNA-seq repeats

A

WT T0 MNase-seq			
	repeat 1	repeat 2	repeat 3
repeat 1	1		
repeat 2	0.82	1	
repeat 3	0.81	0.83	1

B

WT T45 MNase-seq			
	repeat 1	repeat 2	repeat 3
repeat 1	1		
repeat 2	0.84	1	
repeat 3	0.83	0.82	1

C

spt16(G132D) T0 MNase-seq			
	repeat 1	repeat 2	repeat 3
repeat 1	1		
repeat 2	0.7	1	
repeat 3	0.9	0.8	1

D

spt16(G132D) T45 MNase-seq			
	repeat 1	repeat 2	repeat 3
repeat 1	1		
repeat 2	0.9	1	
repeat 3	0.8	0.9	1

E

MNase-seq samples	Correlation between repeats
spt16(G132D)rpb1-1 T0 MNase-seq	0.78
spt16(G132D)rpb1-1 T45 MNase-seq	0.75
rpb1-1 T0 MNase-seq	0.77
rpb1-1 T45 MNase-seq	0.78

F

RNA-seq samples	Correlation between repeats
WT T0 RNA-seq	0.83
WT T45 RNA-seq	0.98
spt16(G132D) T0 RNA-seq	0.84
spt16(G132D) T45 RNA-seq	0.98
spt16(G132D)rpb1-1 T0 RNA-seq	0.84
spt16(G132D)rpb1-1 T45 RNA-seq	0.89
rpb1-1 T0 RNA-seq	0.81
rpb1-1 T45 RNA-seq	0.94

Table S1: MNase-seq datasets and RNA-seq datasets are reproducible.

Wild type or s*pt16 (G132D)* mutant cells at were arrested at G1 at 25°C. These cells were then shifted to 37°C for 45 min (T45) or kept at 25°C (T0). These cells were harvested and subjected to MNase-seq analysis. Nucleosomes were assigned using the

DNAPOS program and the correlation coefficient was calculated based on individual nucleosomes of each repeat. RNA-seq datasets were generated as described in Methods. To calculate correlation coefficient, the expression levels of all genes were calculated, and the correlation coefficient was calculated based on individual genes of each repeat.

Table S2. Total number of reads for each MNase-seq, ChIP-seq and RNA-seq Dataset

samples	sequence type	mapped reads
WT T0 MNase-seq repeat 1	single-end	3913485
WT T0 MNase-seq repeat 2	single-end	2530134
WT T0 MNase-seq repeat 3	single-end	2242105
WT T45 MNase-seq repeat 1	single-end	3718052
WT T45 MNase-seq repeat 2	single-end	5246466
WT T45 MNase-seq repeat 3	single-end	2322472
spt16(G132D) T0 MNase-seq repeat 1	single-end	3987060
spt16(G132D) T0 MNase-seq repeat 2	single-end	4660707
spt16(G132D) T0 MNase-seq repeat 3	single-end	3670763
spt16(G132D) T45 MNase-seq repeat 1	single-end	4271105
spt16(G132D) T45 MNase-seq repeat 2	single-end	2893228
spt16(G132D) T45 MNase-seq repeat 3	single-end	3536522
spt16(G132D)rpb1-1 T0 MNase-seq repeat 1	single-end	2550081
spt16(G132D)rpb1-1 T45 MNase-seq repeat 1	single-end	1708887
spt16(G132D)rpb1-1 T0 MNase-seq repeat 2	paired-end	65170084
spt16(G132D)rpb1-1 T45 MNase-seq repeat 2	paired-end	57986470
rpb1-1 T0 MNase-seq repeat 1	single-end	4036586
rpb1-1 T45 MNase-seq repeat 1	single-end	1511415
rpb1-1 T0 MNase-seq repeat 2	paired-end	72724080
rpb1-1 T45 MNase-seq repeat 2	paired-end	36956710
spt16 TAP tagged ChIP-seq	single-end	2478615
spt16 TAP tagged input	single-end	2048336
w3031a strain spt16 ChIP-seq	single-end	957777
w3031a strain input	single-end	1967069
WT T0 RNA-seq repeat 1	paired-end	19477204
WT T45 RNA-seq repeat 1	paired-end	28839820
spt16(G132D) T0 RNA-seq repeat 1	paired-end	22351150
spt16(G132D) T45 RNA-seq repeat 1	paired-end	30505422
spt16(G132D)rpb1-1 T0 RNA-seq repeat 1	paired-end	24833956
spt16(G132D)rpb1-1 T45 RNA-seq repeat 1	paired-end	26515136
rpb1-1 T0 RNA-seq repeat 1	paired-end	23144076
rpb1-1 T45 RNA-seq repeat 1	paired-end	25695260
WT T0 RNA-seq repeat 2	paired-end	10925128
WT T45 RNA-seq repeat 2	paired-end	31620950
spt16(G132D) T0 RNA-seq repeat 2	paired-end	10034698
spt16(G132D) T45 RNA-seq repeat 2	paired-end	33932212
spt16(G132D)rpb1-1 T0 RNA-seq repeat 2	paired-end	10299394
spt16(G132D)rpb1-1 T45 RNA-seq repeat 2	paired-end	22485392
rpb1-1 T0 RNA-seq repeat 2	paired-end	10261482
rpb1-1 T45 RNA-seq repeat 2	paired-end	20448794

Table S3: Yeast strains used in this study (Isogenic with W303)

Name	Genetic background	Reference
W3031A	*MATa leu2-3, 112 ura3-1 his3-11, 15, trp1-1, ade2-1, can1-100*	(5)
ZGY1059	*MATa leu2-3, 112 ura3-1 his3-11, 15, trp1-1, ade2-1, can1-100, spt16-TAP::TRP*	(6)
ZGY1445	*MATa leu2-3, 112 ura3-1 his3-11, 15, trp1-1, ade2-1, can1-100, spt16 (G132D)*	This study
RS420	*MATa ura3-52, rpb1-1*	(7)
LQY46	*MATa leu2-3, 112 ura3-1 his3-11, 15, trp1-1, ade2-1, can1-100, rpb1-1*	This study
LQY48	*MATa leu2-3, 112 ura3-1 his3-11, 15, trp1-1, ade2-1, can1 100, rpb1-1 spt16 (G132D)*	This study

All yeast strains are in W303 background. Both *spt16 (G132D)* and *rpb1-1* strains were cross with W303 background for more than 4 times before used for the experiments in this study.

Supplemental Methods

Temperature survival assay

To determine the viability of yeast cells in response to the challenge of high temperature treatment, cells were grown in YPD media to log phase, and then arrested in G1 phase using α factor. Equal amounts of yeast cells were subjected to either treatment at 37^{o}C or at 25^{o}C for 45 min. These cells were then diluted and plated onto YPD plates to allow for growing at 25^{o}C for 2-3 days. Colonies were counted, and relative viability was

calculated by the number of colonies formed using cells treated with 37^{o}C divided by that formed without treatment.

Yeast spot assay

To determine whether Spt16-TAP is functional, wild type and *spt16-TAP* strains were challenged using temperature, the agents that affect DNA replication (hydroxyurea (HU)) and transcription (6-Azauracil (6-AU) and mycophenolic acid (MPA). To assay temperature sensitivity, 10-fold serial dilutions of fresh yeast cells were spotted onto non-selective YPD media and incubated at the indicated temperature to assay cell viability. To assay the sensitivity for HU, 10-fold serial dilutions of yeast cells were spotted onto YPD plates containing different concentrations of HU (mM). Plates were incubated at 30^{o}C for at least two days before being photographed using a digital camera (Nikon). To assay 6-AU and MPA sensitivity, wild type and all mutant strains were transformed with pRS316 and grew on SCM-Ura synthetic drop-out plates prior to the test. 10- fold serial dilution of each strain was plated onto SCM-Uracil synthetic drop-out plates containing indicated concentration of different drugs (6-AU dissolved in 1M NH4OH(μg/ml) and MPA dissolved in DMSO (μg/ml)), and was allowed to grow 2-5 days at 25^{o}C before photographs. The experiments were repeated twice and results from a representative single drug concentration were shown.

Supplemental References:

1. **Yu C, Gan H, Han J, Zhou ZX, Jia S, Chabes A, Farrugia G, Ordog T, Zhang Z.** 2014. Strand-Specific Analysis Shows Protein Binding at Replication Forks and PCNA Unloading from Lagging Strands when Forks Stall. Mol Cell **56:**551-563.

2. **David L, Huber W, Granovskaia M, Toedling J, Palm CJ, Bofkin L, Jones T, Davis RW, Steinmetz LM.** 2006. A high-resolution map of transcription in the yeast genome. Proceedings of the National Academy of Sciences of the United States of America **103:**5320-5325.
3. **Foltman M, Evrin C, De Piccoli G, Jones RC, Edmondson RD, Katou Y, Nakato R, Shirahige K, Labib K.** 2013. Eukaryotic replisome components cooperate to process histones during chromosome replication. Cell Rep **3:**892-904.
4. **Anders S, Huber W.** 2010. Differential expression analysis for sequence count data. Genome Biol **11:**R106.
5. **Thomas BJ, Rothstein R.** 1989. Elevated recombination rates in transcriptionally active DNA. Cell **56:**619-630.
6. **Han J, Li Q, McCullough L, Kettelkamp C, Formosa T, Zhang Z.** 2010. Ubiquitylation of FACT by the Cullin-E3 ligase Rtt101 connects FACT to DNA replication. Genes & Development **24:**1485-1490.
7. **Nonet M, Scafe C, Sexton J, Young R.** 1987. Eucaryotic RNA polymerase conditional mutant that rapidly ceases mRNA synthesis. Molecular and Cellular Biology **7:**1602-1611.